Phase-space geometry and reaction dynamics near index 2 saddles

2009 J. Phys. A: Math. Theor. 42 205101

(http://iopscience.iop.org/1751-8121/42/20/205101)

IOP PUBLISHING JOURNAL OF PHYSICS A: MATHEMATICAL AND THEORETICAL

J. Phys. A: Math. Theor. **42** (2009) 205101 (25pp) doi:10.1088/1751-8113/42/20/205101

Phase-space geometry and reaction dynamics near index 2 saddles

Gregory S Ezra[1] **and Stephen Wiggins**[2]

[1] Department of Chemistry and Chemical Biology, Baker Laboratory, Cornell University, Ithaca, NY 14853, USA
[2] School of Mathematics, University of Bristol, Bristol BS8 1TW, UK

E-mail: gse1@cornell.edu and stephen.wiggins@mac.com

Received 24 February 2009, in final form 31 March 2009
Published 5 May 2009
Online at stacks.iop.org/JPhysA/42/205101

Abstract

We study the phase-space geometry associated with index 2 saddles of a potential energy surface and its influence on reaction dynamics for n degree-of-freedom (DoF) Hamiltonian systems. In recent years, similar studies have been carried out for index 1 saddles of potential energy surfaces, and the phase-space geometry associated with classical transition state theory has been elucidated. In this case, the existence of a normally hyperbolic invariant manifold (NHIM) of saddle stability type has been shown, where the NHIM serves as the 'anchor' for the construction of dividing surfaces having the no-recrossing property and minimal flux. For the index 1 saddle case, the stable and unstable manifolds of the NHIM are co-dimension 1 in the energy surface and have the structure of spherical cylinders, and thus act as the conduits for reacting trajectories in phase space. The situation for index 2 saddles is quite different, and their relevance for reaction dynamics has not previously been fully recognized. We show that NHIMs with their stable and unstable manifolds still exist, but that these manifolds by themselves lack sufficient dimension to act as barriers in the energy surface in order to constrain reactions. Rather, in the index 2 case there are different types of invariant manifolds, containing the NHIM and its stable and unstable manifolds, that act as co-dimension 1 barriers in the energy surface. These barriers divide the energy surface in the vicinity of the index 2 saddle into regions of qualitatively different trajectories exhibiting a wider variety of dynamical behavior than for the case of index 1 saddles. In particular, we can identify a class of trajectories, which we refer to as 'roaming trajectories', which are not associated with reaction along the classical minimum energy path (MEP). We illustrate the significance of our analysis of the index 2 saddle for reaction dynamics with two examples. The first involves isomerization on a potential energy surface with multiple (four) symmetry equivalent minima; the dynamics in the vicinity of the saddle enables a rigorous distinction to be made between stepwise (sequential) and concerted (hilltop crossing) isomerization pathways. The second example involves two potential minima connected by

two distinct transition states associated with conventional index 1 saddles, and an index 2 saddle that sits between the two index 1 saddles. For the case of non-equivalent index 1 saddles, our analysis suggests a rigorous dynamical definition of 'non-MEP' or 'roaming' reactive events.

PACS numbers: 05.45.−a, 45.10.Na, 82.20.Db, 82.30.Qt

1. Introduction

Transition state theory has long been and continues to be a cornerstone of the theory of chemical reaction rates [1–6]. In a number of papers in recent years, it has been shown that index 1 saddles[3] of the potential energy surface give rise to a variety of geometrical structures in *phase space*, enabling the realization of Wigner's vision of a transition state theory constructed in *phase space* [7–29].

Following these studies, it is natural to investigate the phase-space structure associated with saddles of index greater than 1 and to elucidate their possible dynamical significance. In this paper, we describe the phase-space structures and their influence on transport in phase space associated with *index 2 saddles* of the potential energy surface for n degree-of-freedom (DoF) deterministic, time-independent Hamiltonian systems.

The phase-space manifestation of an index 1 saddle of the potential energy surface is an equilibrium point of the associated Hamilton's equations of saddle–center–. . .–center stability type. This means that the matrix associated with the linearization of Hamilton's equations about the equilibrium point has one pair of real eigenvalues of equal magnitude, but opposite in sign ($\pm\lambda$) and $n-1$ pairs of purely imaginary eigenvalues, $\pm i\omega_k, k = 2, \ldots, n$.

The phase-space manifestation of an index 2 saddle of the potential energy surface is an equilibrium point of the associated Hamilton's equations of saddle–saddle–center–. . .–center stability type. The matrix associated with the linearization of Hamilton's equations about the equilibrium point then has two pairs of real eigenvalues of equal magnitude, but opposite in sign ($\pm\lambda_1, \pm\lambda_2$) and $n-2$ pairs of purely imaginary eigenvalues, $\pm i\omega_k, k = 3, \ldots, n$[4]. Informally, an index 2 saddle on a potential surface corresponds to a maximum or 'hilltop' in the potential [30–32].

A variety of algorithms exist for determining critical points on potential surfaces [31–33]. The number of higher index critical points on a potential surface must be consistent with the Morse inequalities (provided that the critical points are non-degenerate) [31, 32], and this constraint is often useful in ensuring that all critical points have been located.

It has however been argued that critical points of index 2 and higher are of no direct chemical significance [31, 34]. According to the Murrell–Laidler theorem, if two minima on a potential surface are connected by an index 2 saddle, then there must be a lower energy path between them involving only ordinary transition states (index 1 saddles) [32, 35]. (There are certain well-understood limitations to the Murrell–Laidler theorem [36].) It is therefore true

[3] Consider a potential energy function $V = V(q_1, \ldots, q_n)$ that is a function of n coordinates $\{q_k\}$. (Coordinates describing translation and rotation are excluded.) At a non-degenerate critical point of V, where $\partial V/\partial q_k = 0, k = 1, \ldots, n$, the Hessian matrix $\partial^2 V/\partial q_i \partial q_j$ has n nonzero eigenvalues. The *index* of the critical point is the number of negative eigenvalues.

[4] Without loss of generality, throughout this paper all equilibrium points considered will be located at the origin with zero energy.

that, provided that the reaction coordinate is defined as a minimum energy path (MEP) [31], it cannot pass through an index 2 saddle on a potential surface [32]. If however the reaction coordinate is instead associated with a gradient path (steepest descent/ascent) [34, 37, 38], then it is possible for an index 2 saddle to lie directly on the reaction path [39].

Index 2 saddles (SP 2) were studied in some detail by Heidrich and Quapp [30], who identified two (extreme) classes of SP 2 critical points. The first class, 'virtual' saddles of index 2 (V-SP 2), are associated with two essentially independent index 1 transition states in different parts of a large molecule, and so can be thought of simply as the direct product of two index 1 saddles; an example of a V-SP 2 saddle occurs in the effectively independent internal rotation of the methyl groups in dimethyl ether [40]. In the second class of saddles, 'proper' saddles of index 2 (P-SP 2), the motions associated with the two imaginary vibrational frequencies at the saddle ('downhill' motions) involve the same sets of atoms, and so represent inherently two dimensional dynamical processes.

Examples of proper index 2 potential saddles abound. Heidrich and Quapp discuss the case of face protonated aromatic compounds, where high-energy saddle points of index 2 prevent proton transfer across the aromatic ring, so that proton shifts must occur at the ring periphery [30]. Index 2 saddles are found on potential surfaces located between pairs of minima and index 1 saddles, as in the case of internal rotation/inversion in the H_2BNH_2 molecule [41] or in urea [42], or connected to index 1 saddles connecting four symmetry related minima, as for isomerization pathways in B_2CH_4 [43]. In general, index 2 saddles are found separating symmetry related transition states in so-called 'narcissistic' transformations [44].

It is quite plausible that, for low enough potential barriers [45] or at high enough energies [46], saddles with index >1 might well play a significant role in determining system properties and dynamics. There is for example a continuing debate concerning the role of higher index saddles in determining the behavior of supercooled liquids and glasses [47–55]. Computations on 256 atom LJ binary mixtures [50] show that a significant fraction of saddles with index $\gtrsim 2$ in high-dimensional systems are however 'virtual' saddles in the sense of Heidrich and Quapp [30]. The general relation between configuration space topology (distribution of saddles) and phase transitions is also of great current interest [56]. Several examples of non-MEP or non-IRC reactions [45, 57–62] and 'roaming' mechanisms [63–68] have been identified in recent years; the dynamics of these reactions is not mediated by a single conventional transition state associated with an index 1 saddle. Higher index saddles can also become mechanistically important for structural transformations of atomic clusters [69] when the range of the pairwise potential is reduced [70].

Earnshaw's theorem [71] suggests that higher index saddles are likely to be ubiquitous in classical models of atoms and molecules, where all particles interact via the Coulomb potential. The role of index 2 saddles in the (classical) ionization dynamics of the Helium atom in an external electric field [72–74] has in fact recently been studied from a phase-space perspective by Haller, Palacian, Yanguas, Uzer and Jaffe [75].

Index 2 saddles have been mentioned by Toda, Komatsuzaki and coworkers in the context of the breakdown of normal hyperbolicity in NHIMs associated with index 1 saddles, as a result of chaotic motions within the NHIM [76–78]. Specifically, the index 2 saddle has been proposed as a model for phase-space structure in the vicinity of a particular unstable periodic orbit in the NHIM [78].

Phase-space structures and their influence on phase-space transport were developed in some detail for the case of an index 1 saddle of the potential energy surface (henceforth, 'index 1 saddles') corresponding to an equilibrium point of saddle–center–. . .–center stability type for the corresponding Hamilton's equations [9]. In this paper, we follow a similar path

for index 2 saddles. (A generalization of phase-space transition state theory from index 1 to higher index saddles has independently been given by Haller *et al* [75].)

The outline for this paper is as follows. We begin in section 2 by discussing the phase-space structure of the inverted parabolic barrier, an index 1 saddle. This elementary example provides the foundation for our treatment of higher index saddles. In section 3, we consider geometry and transport associated with a 3 DoF quadratic Hamiltonian for a saddle–saddle–center. This simple model contains the essential features of the problem we are considering. The quadratic Hamiltonian is separable (and integrable), and we can therefore consider the saddle–saddle dynamics and center dynamics separately. The saddle–saddle dynamics is considered in detail in section 3.2, where we show that the two integrals associated with the saddle–saddle dynamics serve to classify the geometry of trajectories that pass through a neighborhood of the saddle–saddle. This 'reduced dimensionality' analysis of the saddle–saddle dynamics associated with separability of the quadratic Hamiltonian is central to our analysis. We introduce a symbolic representation of the qualitatively distinct classes of trajectory behavior in the vicinity of the saddle–saddle equilibrium and show that this symbolic representation can be placed into direct correspondence with the different classes of trajectories in the vicinity of the potential hilltop.

For completeness, and in analogy with the 3 DoF case, we consider a quadratic n DoF model of a Hamiltonian having an equilibrium point of saddle–saddle–center–. . .–center equilibrium type in the appendix and show that separability of the quadratic Hamiltonian implies that the 3 DoF analysis easily goes though for the n DoF case, with obvious modifications. In section 4, we consider the general case of a n DoF fully nonlinear Hamiltonian having an equilibrium point of saddle–saddle–center–. . .–center stability type. In a neighborhood of the equilibrium point the Poincaré–Birkhoff normal form theory can be applied to construct a set of new coordinates in which the Hamiltonian assumes a simple form (which we describe). In fact, for generic non-resonance conditions on the eigenvalues of the matrix associated with the linearization of Hamilton's equations about the equilibrium point, the normal form Hamiltonian is integrable. We show that integrability provides all of the advantages that separability provided for the quadratic Hamiltonians: the saddle–saddle dynamics can be described separately and the two integrals associated with the saddle DoFs can be used to characterize completely the geometry of trajectories passing through a neighborhood of the saddle–saddle–center–. . .–center equilibrium point.

As for the case of index 1 saddles, normally hyperbolic invariant manifolds (NHIMs) [7, 79] associated with index 2 saddles are an important phase-space structure and we describe the nature of their existence and the role they play in phase-space transport in the vicinity of index 2 saddles in section 5.

In section 6, we discuss two examples where the phase-space structure in the vicinity of an index 2 saddle is potentially of importance in a problem of chemical dynamics. The first example involves isomerization on a potential energy surface with multiple (four) symmetry equivalent minima; the dynamics in the vicinity of the index 2 saddle enables a rigorous distinction to be made between stepwise (sequential) and concerted (hilltop crossing) isomerization pathways [45]. In the second example, two potential minima are connected by two distinct transition states associated with conventional index 1 saddles, and an index 2 saddle sits between the two index 1 saddles. (The transition states do not have to be symmetry equivalent [44].) For high enough energies, analysis of the phase-space geometry in the vicinity of the index 2 saddle enables different classes of reactive trajectories to be distinguished. In particular, for the case of non-equivalent index 1 saddles, we can rigorously define 'non-MEP' or 'roaming' events. Section 7 concludes with a discussion of some outstanding problems for future investigation.

2. Index 1 saddle: inverted harmonic oscillator

In this section, we give a quantitative description of trajectories passing through a neighborhood of an equilibrium point of saddle stability type (in brief, a 'saddle') for 1 DoF Hamiltonian systems. While the basic material is of course well known, our discussion will illustrate the distinction between physical coordinates and normal form coordinates, show how an integral is used to distinguish qualitatively different trajectories that pass through a neighborhood of the saddle and develop a symbolic description that describes the qualitatively distinct trajectories that pass through a neighborhood of the saddle. Establishing these ideas in this simple case will allow for a straightforward generalization to more DoF, beginning in section 3.

We consider the problem of a one-dimensional inverted harmonic oscillator (negative parabolic potential), which in suitably scaled physical coordinates $(\bar{q}_1, \bar{p}_1)$ corresponds to the Hamiltonian

$$h_1 = \frac{\lambda_1}{2}\left(\bar{p}_1^2 - \bar{q}_1^2\right), \tag{1}$$

with $\lambda_1 > 0$. In general, a Hamiltonian of this form provides an approximate description of motion in the vicinity of the top of a (generic, non-degenerate) one-dimensional barrier. The canonical transformation $(\bar{q}_1, \bar{p}_1) \mapsto (q_1, p_1)$, where

$$\bar{p}_1 = \tfrac{1}{\sqrt{2}}(q_1 + p_1) \tag{2a}$$

$$\bar{q}_1 = \tfrac{1}{\sqrt{2}}(q_1 - p_1), \tag{2b}$$

transforms the inverted harmonic oscillator Hamiltonian (1) into the normal form

$$h_1 = \lambda_1 p_1 q_1. \tag{3}$$

The associated equations of motion in normal form coordinates are

$$\dot{q}_1 = \frac{\partial h_1}{\partial p_1} = \lambda_1 q_1 \tag{4a}$$

$$\dot{p}_1 = -\frac{\partial h_1}{\partial q_1} = -\lambda_1 p_1 \tag{4b}$$

with solutions

$$q_1 = q_1^0 \, \mathrm{e}^{+\lambda_1 t} \tag{5a}$$

$$p_1 = p_1^0 \, \mathrm{e}^{-\lambda_1 t}. \tag{5b}$$

The phase-space origin ($\bar{q}_1 = 0$, $\bar{p}_1 = 0$) is therefore an equilibrium point of saddle type. Phase-space portraits for the inverted harmonic oscillator in terms of the physical variables $(\bar{q}_1, \bar{p}_1)$ and the normal form variables (q_1, p_1) are shown in figure 1. We remark that the canonical (or symplectic) transformation to normal form coordinates and the Hamiltonian expressed in these coordinates (known as the 'normal form Hamiltonian') are trivial in this 1 DoF case. The real power of the normal form approach becomes clear for 2 and more DoF where it is a simple matter to describe trajectories near a higher dimensional 'saddle', and the phase-space structures near the saddle can easily be described in terms of (approximate) integrals and the normal form coordinates (see [16] and references therein).

The Hamiltonian (3) can be written in terms of the action variable

$$I_1 = p_1 q_1 \tag{6}$$

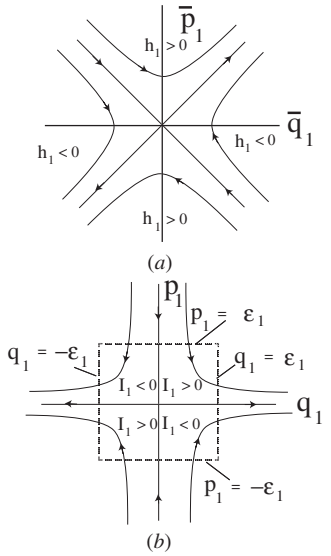

Figure 1. The phase-space geometry associated with the inverted parabolic potential in (*a*) physical coordinates and (*b*) normal form coordinates.

which is obviously a conserved quantity (proportional to the Hamiltonian h_1). The action I_1 can be positive, negative or zero.

The condition $I_1 = 0$ defines 2 co-dimension one[5] invariant manifolds ($p_1 = 0$ and $q_1 = 0$) that intersect at the saddle equilibrium point, which is the most basic example of a NHIM. More importantly, these invariant manifolds divide the phase plane into four regions (quadrants) corresponding to qualitatively different types of trajectories.

In terms of the *physical* variables ($\bar{q}_1$, $\bar{p}_1$), the two quadrants with $I_1 > 0$ are associated with motions where the particle has enough energy to surmount the top of the parabolic barrier, so that there is no turning point in the coordinate $\bar{q}_1$ (classical barrier transmission), whereas the two quadrants for which the action $I_1 < 0$ are associated with motions for which the particle has insufficient energy to surmount the barrier, so that the coordinate $\bar{q}_1$ exhibits a turning point (classical reflection from barrier).

To obtain a more precise classification of the possible motions in the vicinity of the equilibrium point, we define a phase-space neighborhood $\mathcal{N}$ of the equilibrium point as follows:

$$\mathcal{N} \equiv \{(q_1, p_1) \mid |q_1| \leqslant \varepsilon_1, |p_1| \leqslant \varepsilon_1\}, \tag{7}$$

for some suitably chosen ε_1.[6] A trajectory enters $\mathcal{N}$ if at some time it crosses the boundary of $\mathcal{N}$ with the velocity vector pointing into $\mathcal{N}$. Similarly for trajectories that exit $\mathcal{N}$. It is easy to see from (5) that, with the exception of the (zero Lebesgue measure) set of trajectories that enter $\mathcal{N}$ with $|q_1| = 0$, all trajectories that enter $\mathcal{N}$ exit $\mathcal{N}$. In fact, we can characterize the condition for entry and exit of trajectories to and from $\mathcal{N}$ as follows:

[5] Briefly, the co-dimension of a manifold is the dimension of the space in which the manifold exists, minus the dimension of the manifold. The significance of a manifold being 'co-dimension 1' is that it is one less dimension than the space in which it exists. Therefore it can 'divide' the space and act as a separatrix, or barrier, to transport. Co-dimension two manifolds do not have this property.

[6] For the quadratic Hamiltonians, we consider ε_1 (and ε_2) can be chosen $\mathcal{O}(1)$. When Hamiltonians with higher order terms are considered, a more careful consideration of the size of ε_1 and ε_2 is required.

Condition for entry into $\mathcal{N}$: $|p_1(0)| = \varepsilon_1$, $|I_1| < \varepsilon_1^2$.
Condition for exit from $\mathcal{N}$: $|q_1(0)| = \varepsilon_1$, $|I_1| < \varepsilon_1^2$.

Trajectories that exit and enter $\mathcal{N}$ remain in the same quadrant in the (q_1, p_1) plane, and either pass over or are reflected by the potential barrier (this latter interpretation is based on the Hamiltonian expressed in terms of the physical coordinates). Corresponding to the four distinct quadrants, we define four classes of trajectory:

- (++) ($q_1 > 0$, $p_1 < 0$),
- (−+) ($q_1 < 0$, $p_1 < 0$),
- (+−) ($q_1 > 0$, $p_1 > 0$),
- (−−) ($q_1 < 0$, $p_1 > 0$).

This description uses both the physical and normal form coordinates, and the notation indicates the net result of passage through region $\mathcal{N}$ in terms of the action of an associated 'scattering map'. Considering the first item, reading from right to left[7], (+, +) refers to a trajectory in the physical coordinates that enters the neighborhood of the saddle with $\bar{q}_1 > 0$ and exits the neighborhood of the saddle with $\bar{q}_1 > 0$, i.e. it is reflected from the barrier on the $\bar{q}_1 > 0$ side. In the normal form coordinates, this trajectory corresponds to a trajectory in the fourth quadrant, ($q_1 > 0$, $p_1 < 0$). Similarly, trajectories of type (−+) enter a neighborhood of the saddle with $\bar{q}_1 > 0$, pass over the saddle and exit the neighborhood of the saddle with $\bar{q}_1 < 0$. In normal form coordinates, these correspond to trajectories in the third quadrant, ($q_1 < 0$, $p_1 < 0$). The remaining two cases are understood similarly.

3. Phase-space geometry and transport associated with a 3 DoF quadratic Hamiltonian of a saddle–saddle–center equilibrium

In this section, we describe the nature of trajectories as they pass through a neighborhood of an index 2 saddle for a 3 DoF quadratic Hamiltonian. We will express the Hamiltonian in normal form coordinates. However, the symbolic representation of the trajectories will be based on dynamics described in terms of the physical coordinates, as in the previous section.

3.1. Quadratic saddle–saddle–center system

We now consider a 3 DoF quadratic Hamiltonian that describes the dynamics near a saddle–saddle–center stability type equilibrium point located at the origin:

$$H_{\text{ssc}} = \lambda_1 q_1 p_1 + \lambda_2 q_2 p_2 + \frac{\omega}{2}\left(q_3^2 + p_3^2\right), \qquad \lambda_1, \lambda_2, \omega > 0. \tag{8}$$

Note that the variables (q_1, p_1, q_2, p_2) in the Hamiltonian (8) are not physical coordinates, but rather normal form coordinates as defined in equation (2). The Hamiltonian (8) can be used to describe dynamics in the vicinity of a hilltop (non-degenerate index 2 saddle) in a three-dimensional potential energy surface.

The Hamiltonian (8) is completely integrable, with (independent) integrals:

$$I_1 = q_1 p_1, \qquad I_2 = q_2 p_2, \qquad I_3 = \tfrac{1}{2}\left(q_3^2 + p_3^2\right), \tag{9}$$

and can be expressed as a function of the integrals:

$$H_{\text{ssc}} = \lambda_1 I_1 + \lambda_2 I_2 + \omega I_3. \tag{10}$$

These integrals play a crucial role in our understanding of the underlying phase-space geometry and transport.

[7] The notational convention used here is inspired by quantum mechanics: if the initial (incident) state is denoted by i, the final (scattered) state is denoted by f, the quantum mechanical scattering amplitude is given by the matrix element $\langle f|\hat{S}|i\rangle$, with $\hat{S}$ being the scattering operator. The transition associated with the scattering event is then $f \leftarrow i$.

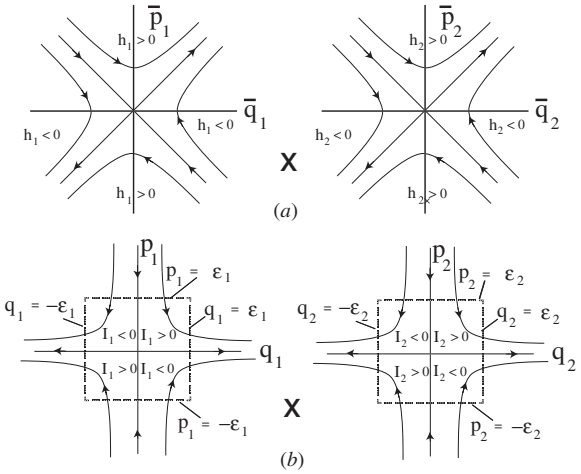

Figure 2. The geometry associated with the 2 DoF saddle–saddle subsystem.

3.2. Phase-space geometry and transport associated with the 2 DoF saddle–saddle subsystem

An important consequence of the separability of the 3 DoF quadratic Hamiltonian (8) is that an understanding of the nature of the trajectories passing through a neighborhood of the saddle–saddle–center equilibrium point can be obtained through a study of the 2 DoF subsystem corresponding to the saddle–saddle, since motion in the center DoF is bounded and the action I_3 is conserved. The Hamiltonian for this 2 DoF subsystem is

$$H_{\rm ss} = \lambda_1 q_1 p_1 + \lambda_2 q_2 p_2, \tag{11}$$

with integrals I_1 and I_2 as given in (9).

Hamilton's equations for the 2 DoF saddle–saddle subsystem are given by

$$\dot{q}_1 = \frac{\partial H_{\rm ss}}{\partial p_1} = \lambda_1 q_1, \tag{12a}$$

$$\dot{p}_1 = -\frac{\partial H_{\rm ss}}{\partial q_1} = -\lambda_1 p_1, \tag{12b}$$

$$\dot{q}_2 = \frac{\partial H_{\rm ss}}{\partial p_2} = \lambda_2 q_2, \tag{12c}$$

$$\dot{p}_2 = -\frac{\partial H_{\rm ss}}{\partial q_2} = -\lambda_2 p_2. \tag{12d}$$

The phase flow in the vicinity of the saddle–saddle equilibrium is shown in figure 2. In this figure, we show the phase flow in both the physical coordinates defined in (1) and the normal form coordinates. The transformation between these two sets of coordinates is given in (2). Since our Hamiltonian is separable, it is a trivial matter to use this coordinate transformation on both saddles to express the Hamiltonian in physical coordinates. However, the separability also means that we can immediately adapt the discussion of the previous section for physical coordinates to the saddle–saddle case, and it is this approach that we will follow.

As before, we define a neighborhood $\mathcal{N}$ of the equilibrium point in phase space as follows:

$$\mathcal{N} \equiv \{(q_1, p_1, q_2, p_2) \mid |q_1| \leqslant \varepsilon_1, |p_1| \leqslant \varepsilon_1, |q_2| \leqslant \varepsilon_2, |p_2| \leqslant \varepsilon_2\}, \tag{13}$$

for some suitably chosen ε_1 and ε_2.[8] As for the 1 DoF case, with the exception of the (zero Lebesgue measure) set of trajectories that enter $\mathcal{N}$ with $|q_1| = |q_2| = 0$, all trajectories that enter $\mathcal{N}$, exit $\mathcal{N}$. We characterize the condition for entry and exit of trajectories to and from $\mathcal{N}$ as follows:

Condition for entry into $\mathcal{N}$: $|p_1(0)| = \varepsilon_1, |p_2(0)| = \varepsilon_2, |I_1 I_2| < \varepsilon_1^2 \varepsilon_2^2$.
Condition for exit from $\mathcal{N}$: $|q_1(0)| = \varepsilon_1, |q_2(0)| = \varepsilon_2, |I_1 I_2| < \varepsilon_1^2 \varepsilon_2^2$.

As for the 1 DoF unstable equilibrium, we can define different classes of trajectories characterized by their behavior under the scattering map corresponding to passage through the region $\mathcal{N}$. For the 2 DoF case, there are $4 \times 4 = 16$ combinations of quadrants and 16 types of trajectories. The symbolic description of the behavior of a trajectory as it passes through a neighborhood of the saddle–saddle with respect to the physical coordinates $\bar{q}_k, k = 1, 2$, is expressed by the following four symbols, $(f_1 f_2; i_1 i_2)$, where $i_1 = \pm, i_2 = \pm, f_1 = \pm, f_2 = \pm$. Here $i_k, k = 1, 2$ refer to the 'initial' sign of $\bar{q}_k, k = 1, 2$ as it enters the neighborhood of the saddle–saddle and $f_k, k = 1, 2$ refer to the 'final' sign of $\bar{q}_k, k = 1, 2$, as it leaves the neighborhood of the saddle. For example, trajectories of class $(--; +-)$ pass over the barrier from $\bar{q}_1 > 0$ to $\bar{q}_1 < 0$, but remain on the side of the barrier with $\bar{q}_2 < 0$.

Of the 16 qualitatively distinct classes of trajectories, the four types $(++; --)$, $(-+; +-)$, $(+-; -+)$ and $(--; ++)$ are the only trajectories that undergo a change of sign of both coordinates $\bar{q}_1$ and $\bar{q}_2$, and so they are the trajectories that pass 'over the hilltop' in the vicinity of the saddle–saddle equilibrium.

As in the 1 DoF case, co-dimension 1 surfaces separate the different types of trajectories. These are the four co-dimension 1 invariant manifolds given by $q_1 = 0$, $p_1 = 0$, $q_2 = 0$, $p_2 = 0$ (i.e. $I_1 = 0$, $I_2 = 0$). For example, the co-dimension 1 surface $q_1 = 0$ forms the boundary between trajectories of types $(++; +-)$ and $(-+; +-)$, and so on.

The dynamical significance of this symbolic classification is discussed in section 6 in the context of isomerization reactions.

3.3. Including the additional center DoF

Because the system is separable, including the additional center DoF has no effect on our discussion above on the nature of trajectories in the 2 DoF saddle–saddle subsystem as they pass through a neighborhood of the saddle.

To see this, note that equations of motion for the Hamiltonian (11) are given by

$$\dot{q}_1 = \frac{\partial H_{\text{ssc}}}{\partial p_1} = \lambda_1 q_1, \tag{14a}$$

$$\dot{p}_1 = -\frac{\partial H_{\text{ssc}}}{\partial q_1} = -\lambda_1 p_1, \tag{14b}$$

$$\dot{q}_2 = \frac{\partial H_{\text{ssc}}}{\partial p_2} = \lambda_2 q_2, \tag{14c}$$

$$\dot{p}_2 = -\frac{\partial H_{\text{ssc}}}{\partial q_2} = -\lambda_2 p_2, \tag{14d}$$

[8] See footnote 6.

$$\dot{q}_3 = \frac{\partial H_{\rm ssc}}{\partial p_3} = \omega p_3, \tag{14e}$$

$$\dot{p}_3 = -\frac{\partial H_{\rm ssc}}{\partial q_3} = -\omega q_3. \tag{14f}$$

As previously, we define a neighborhood of the saddle–saddle–center equilibrium point in phase space as follows:

$$\mathcal{N} \equiv \{(q_1, p_1, q_2, p_2, q_3, p_3) \mid |q_1| \leqslant \varepsilon_1, |p_1| \leqslant \varepsilon_1, |q_2| \leqslant \varepsilon_2, |p_2| \leqslant \varepsilon_2 |q_3| \leqslant \varepsilon_3, |p_3| \leqslant \varepsilon_3\}, \tag{15}$$

for suitably chosen ε_1, ε_2 and ε_3. We want to describe the geometry associated with trajectories that enter and leave $\mathcal{N}$. First, note again the fact that Hamilton's equations are separable and that the (simple harmonic) motion of q_3 and p_3 is bounded. It then follows that if q_3 and p_3 are initially chosen to satisfy the condition for being in $\mathcal{N}$, then they satisfy this condition for all the time. Hence, the issue of trajectories entering $\mathcal{N}$ and exiting $\mathcal{N}$ depends entirely on the behavior of the (q_1, p_1, q_2, p_2) components of a trajectory and, as a consequence of separability, this behavior is exactly as described in section 3.2.

We now examine some further aspects of the geometry for the 3 DoF quadratic Hamiltonian model of a saddle–saddle–center. The equilibrium point is located at the origin and has zero energy. We consider geometric structures in the energy surface for positive energies:

$$H_{\rm ssc} = \lambda_1 q_1 p_1 + \lambda_2 q_2 p_2 + \frac{\omega}{2}\left(q_3^2 + p_3^2\right) = E > 0. \tag{16}$$

It is clear from (14) that $q_1 = p_1 = q_2 = p_2 = 0$ is a two-dimensional invariant manifold in the six-dimensional phase space. Using (16), its intersection with the five-dimensional energy surface is given by

$$\frac{\omega}{2}\left(q_3^2 + p_3^2\right) = E > 0. \tag{17}$$

This is a periodic orbit in the energy surface but, more generally, it is an example of a NHIM. The coordinates q_1, p_1, q_2, p_2 can be viewed as coordinates for the normal directions of the NHIM, and it follows from the nature of the asymptotic (in time) behavior of these coordinates (see (14)) that this NHIM has a three-dimensional stable manifold and a three-dimensional unstable manifold in the five-dimensional energy surface. Further discussion of the role of NHIMs is given in section 5.3.

4. *n* DoF, higher order terms in the Hamiltonian, and the Poincaré–Birkhoff normal form

The examples we have considered so far have been exceptional—quadratic, separable—Hamiltonians (which implies that they are completely integrable). Now we will show that for a general time-independent Hamiltonian, in a neighborhood of an equilibrium point of saddle–saddle–center–. . .–center stability type, a 'good set of coordinates' can be found in terms of which the Hamiltonian assumes a simple form for which the results described above hold. Moreover, these coordinates are obtained via a constructive algorithm.

For completeness, in the appendix we consider in detail the nature of trajectories associated with a quadratic n DoF Hamiltonian model that describes the dynamics near a saddle–saddle–center–. . .–center stability type equilibrium point, and then we consider the case where higher order terms are included in this model.

4.1. Normal form for n DoF

Specifically, in a neighborhood of an equilibrium point of saddle–saddle–center–. . .–center stability type, the Poincaré–Birkhoff normal form theory can be used to (formally) construct a symplectic change of coordinates so that in the new coordinates the Hamiltonian has the form

$$H = \lambda_1 q_1 p_1 + \lambda_2 q_2 p_2 + \sum_{i=3}^{n} \frac{\omega_i}{2}\left(q_i^2 + p_i^2\right) + f(q_1, \ldots, q_n, p_1, \ldots, p_n), \tag{18}$$

where $f(q_1, \ldots, q_n, p_1, \ldots, p_n)$ assumes a particularly simple form that is amenable to analysis. This is discussed in some detail, with particular relevance to reaction dynamics, in [16]. For our purposes, if we assume that the purely imaginary eigenvalues satisfy the non-resonance condition $k_3\omega_3 + \ldots + k_n\omega_n \neq 0$ for any $n-2$ vector of integers $(k_3, \ldots, k_n)$ with *not all* $k_i = 0$ (that is, $(k_3, \ldots, k_n) \in \mathbb{Z}^{n-2} - \{0\}$) and the real eigenvalues satisfy the (independent) non-resonance condition $k_1\lambda_1 + k_2\lambda_2 \neq 0$ for any 2 vector of integers (k_1, k_2) with *not all* $k_i = 0, i = 1, 2$, then $f(q_1, \ldots, q_n, p_1, \ldots, p_n)$ can be represented as an even order polynomial in the variables

$$I_1 = q_1 p_1, \qquad I_2 = q_2 p_2, \qquad I_k = \frac{\omega_k}{2}\left(q_k^2 + p_k^2\right), \qquad k = 3, \ldots, n. \tag{19}$$

In other words, we can express the normal form Hamiltonian in this situation as[9]

$$H(I_1, I_2, I_3, \ldots, I_n), \tag{20}$$

with the associated Hamilton's equations given by

$$\dot{q}_1 = \frac{\partial H}{\partial p_1} = \frac{\partial H}{\partial I_1}\frac{\partial I_1}{\partial p_1} = \frac{\partial H}{\partial I_1} q_1, \tag{21a}$$

$$\dot{p}_1 = -\frac{\partial H}{\partial q_1} = -\frac{\partial H}{\partial I_1}\frac{\partial I_1}{\partial q_1} = -\frac{\partial H}{\partial I_1} p_1, \tag{21b}$$

$$\dot{q}_2 = \frac{\partial H}{\partial p_2} = \frac{\partial H}{\partial I_2}\frac{\partial I_2}{\partial p_2} = \frac{\partial H}{\partial I_2} q_2, \tag{21c}$$

$$\dot{p}_2 = -\frac{\partial H}{\partial q_2} = -\frac{\partial H}{\partial I_2}\frac{\partial I_2}{\partial q_2} = -\frac{\partial H}{\partial I_2} p_2, \tag{21d}$$

$$\dot{q}_k = \frac{\partial H}{\partial p_k} = \frac{\partial H}{\partial I_k}\frac{\partial I_k}{\partial p_k} = \frac{\partial H}{\partial I_k} p_k, \tag{21e}$$

$$\dot{p}_k = -\frac{\partial H}{\partial q_k} = -\frac{\partial H}{\partial I_k}\frac{\partial I_k}{\partial q_k} = -\frac{\partial H}{\partial I_k} q_k, \qquad k = 3, \ldots, n, \tag{21f}$$

and it can be verified by a direct calculation that $I_k, k = 1, \ldots, n$ are integrals of the motion for (21).[10]

[9] The normal form for the saddle–saddle–center–. . .–center has not received a great deal of individual attention in the literature. Nevertheless, this particular form of the normal form has been well known for some time. See, for example, [85, 86]. See also the documentation of the normal form software available at http://lacms.maths.bris.ac.uk/publications/software/index.html.

[10] The normal form algorithm operates in an iterative fashion by simplifying terms in the Taylor expansion about the equilibrium point 'order by order', i.e. the order M terms are normalized, then the order $M+1$ terms are normalized, etc. The algorithm is such that normalization at order M does not affect any of the lower order terms (which have already been normalized). The point here is that although the algorithm can be carried out to arbitrarily high order, practically we must stop the normalization at some order (i.e. truncate the Hamiltonian). In practice, we have found that truncations of the normal form Hamiltonian can be extremely accurate according to various tests which we discuss in section 4.2.

Since $I_k, k = 1, \ldots, n$ are constant on trajectories, it follows that the partial derivatives $\frac{\partial H}{\partial I_k}, k = 1, \ldots, n$ are also constant on trajectories. Hence, it follows that the structure of equations (21) is extremely simple, and this is a consequence of the integrability of the normal form.

The possible role of resonances (commensurabilities) between the saddle eigenvalues λ_i in the breakdown of normal hyperbolicity in NHIMs has been discussed by Toda, Komatsuzaki and coworkers [76–78]. Here, we assume that such resonances are not present; in particular, we assume $\lambda_1 \neq \lambda_2$.

We can define a neighborhood of the equilibrium point exactly as in equation (A.3) in the appendix and consider the geometry associated with trajectories that enter and leave $\mathcal{L}$. Even though the nonlinear Hamilton's equations (21) are *not* separable, it follows from integrability and the structure of (21) that the motion of q_k and p_k is bounded, $k = 3, \ldots, n$ (q_k and p_k just undergo periodic motion, individually for each k, although the frequency of motion can vary from trajectory to trajectory). It then follows that if q_k and $p_k, k = 3. \ldots, n$, are initially chosen in $\mathcal{L}$, then they remain in $\mathcal{L}$ for all the time. Hence, exactly as in the quadratic case, the issue of trajectories entering $\mathcal{L}$ and exiting $\mathcal{L}$ depends entirely on the behavior of the (q_1, p_1, q_2, p_2) components of a trajectory and, as a consequence of integrability, this behavior is exactly as described in section 3.2 and we have the integrals I_1 and I_2 as parameters for describing the geometry of the trajectories during their passage though $\mathcal{L}$.

Exactly as for the model quadratic Hamiltonians, it is simple to verify that $q_1 = p_1 = q_2 = p_2 = 0$ is a $(2n-4)$-dimensional invariant manifold in the $2n$-dimensional phase space. For energies greater than zero (the energy of the saddle–saddle–center–. . .–center), in the $(2n-1)$-dimensional energy surface it is a $(2n-5)$-dimensional NHIM with $(2n-3)$-dimensional stable and unstable manifolds (they are co-dimension two[11] in the energy surface). An important property of NHIMs is that they, as well as their stable and unstable manifolds, persist under perturbation. If we consider a small $\mathcal{L}$, then the terms $f(q_1, p_1, \ldots, q_n, p_n)$ can be considered as a perturbation of the quadratic Hamiltonian, for which the NHIM had the geometrical structure of S^{2n-5}. If the perturbation is 'sufficiently small' then this spherical structure is preserved.

4.2. Accuracy of the normal form

The normalization proceeds via formal power series manipulations whose input is a Taylor expansion of the original Hamiltonian, H, necessarily up to some finite order, M, in homogeneous polynomials. For a particular application, this procedure naturally necessitates a suitable choice of the order, M, for the normalization, after which one must make a restriction on some local region, $\mathcal{L}$, about the equilibrium point in which the resulting computations achieve some desired accuracy. Hence, the accuracy of the normal form as a power series expansion truncated at order M in a neighborhood $\mathcal{L}$ is determined by comparing the dynamics associated with the normal form with the dynamics of the original system. There are several independent tests that can be carried out to verify the accuracy of the normal form. Straightforward tests that we have used are the following [10, 12–14, 16, 80]:

- Examine how the integrals associated with the normal form change on trajectories of the full Hamiltonian (the integrals will be constant on trajectories of the normal form).
- Check the invariance of the different invariant manifolds (i.e., the NHIM and its stable and unstable manifolds) with respect to trajectories of the full Hamiltonian.

[11] See footnote 5.

Both of these tests require us to use the transformations between the original coordinates and the normal form coordinates. Specific examples where M, $\mathcal{L}$ and accuracy of the normal forms and the constancy of integrals of the truncated normal form are considered can be found in [10, 12–14, 80]. A general discussion of the accuracy of the normal form can be found in [16].

5. Comparison of phase-space geometry and trajectories for index 1 and index 2 saddles

In this section, we discuss a number of issues that arise from the above results and discussions. For comparative purposes, it is helpful first to summarize the nature of trajectories that pass near an index 1 saddle and trajectories that pass near an index 2 saddle.

5.1. Index 1 saddles

For index 1 saddles, it was shown in previous work that for energies above that of the saddle–center–. . .–center there exists a $(2n-3)$-dimensional normally hyperbolic invariant manifold (NHIM) in the $(2n-1)$-dimensional energy surface [7, 9, 79]. The NHIM is of saddle stability type and has $(2n-2)$-dimensional stable and unstable manifolds. Since these are one less dimension than the energy surface, they act as higher dimensional separatrices and serve to partition phase space into regions corresponding to qualitatively different types of trajectories:

- forward reactive trajectories $\equiv (+-)$,
- forward non-reactive trajectories $\equiv (--)$,
- backward reactive trajectories $\equiv (-+)$,
- backward non-reactive trajectories $\equiv (++)$,

where we have indicated the correspondence with the trajectory classification introduced in section 2.

The NHIM is the 'anchor' for the construction of a phase-space dividing surface having the geometrical structure of a $(2n-2)$-dimensional sphere. The NHIM is the equator of this $(2n-2)$-dimensional sphere, hence dividing it into two hemispheres. Forward reacting trajectories pass through one hemisphere and backward reacting trajectories pass through the other hemisphere. These 'dividing hemispheres' have the *no-recrossing property* in the sense that the vector field defined by Hamilton's equations is strictly transverse to each hemisphere. Moreover, the magnitude of the flux is minimal (and equal) for each hemisphere.

The language used for the description of trajectories for the case of an index 1 saddle is that of reaction. Trajectories evolve from reactants to products by passing through a dividing surface that locally 'divides' the energy surface into two disjoint pieces–reactants and products.

Here, we have classified trajectories in the vicinity of an index 1 saddle in a slightly less general but more explicit fashion in terms of their behavior with respect to crossing a potential barrier; this classification is useful in the treatment of reactive dynamics in the vicinity of higher index saddles on potential energy surfaces, as discussed below.

5.2. Index 2 saddles

The geometrical structures associated with index 1 saddles provide a rigorous way of partitioning the phase space into regions that describe the evolution of a system from reactants to products by passing through a dividing surface having the no-recrossing and minimal flux properties. This partitioning is made possible by the existence of invariant manifolds that have the proper dimension and stability type. Moreover, their geometric character is such

that the partitioning that they provide has the natural interpretation of regions of reactants and products of the energy surface, and the stable and unstable manifolds of the NHIM provide natural boundaries between these regions.

For index 2 saddles the same types of invariant manifolds still exist—a NHIM and co-dimension 1 (in the energy surface) invariant manifolds. These co-dimension 1 invariant manifolds ($q_i = 0$, $p_i = 0, i = 1, 2$) were introduced above and are discussed further below. It was shown that the passage of trajectories through the neighborhood of the equilibrium could be understood in terms of a 2 DoF saddle–saddle subsystem and values of the two associated action integrals.

For index 2 saddles, all trajectories (except for the set of Lebesgue measure zero discussed above) that enter the neighborhood of the equilibrium point exit the neighborhood of the equilibrium point, and there are 16 qualitatively different types of trajectories that enter and exit this neighborhood. These sixteen classes are characterized by their crossing behavior with respect to the 'hilltop' in the potential surface associated with the index 2 saddle.

Two examples involving isomerization reactions where this classification of trajectories is of chemical relevance are discussed in section 6.

5.3. The role of NHIMs and the existence of co-dimension 1 invariant manifolds in the energy surface

It has previously been argued [9] that the invariant manifold structure associated with index 1 saddles is a natural generalization to 3 or more DoF of the PODS, and their associated invariant manifolds, where the latter have provided a fundamental understanding of transition state theory for systems with 2 DoF [3]. The necessary ingredient to make the leap from 2 DoF to higher DoF is the realization that a NHIM of saddle stability type is the natural generalization to higher DoF of the periodic orbit of saddle stability type familiar from 2 DoF [9, 81]. The resulting geometric picture of reaction for $N > 2$ DoF is essentially that of the 2 DoF case, the key feature of the generalization being the availability of the necessary invariant manifolds to partition the energy surface in the multidimensional case in a manner that is meaningful for reaction.

The situation with index 2 saddles is fundamentally different. On energy surfaces above that of the saddle, a NHIM still exists, but it is co-dimension 4 in the energy surface with co-dimension 2 stable and unstable manifolds. Nevertheless, as shown above, it is still possible to construct co-dimension 1 invariant manifolds (in the energy surface) that locally partition the energy surface into regions associated with qualitatively different types of trajectories passing through a neighborhood of the equilibrium point: the surfaces defined by the conditions $q_1 = 0$, $p_1 = 0$ $q_2 = 0$ and $p_2 = 0$ are each co-dimension 1 invariant manifolds in the $2n$-dimensional phase space, and they are also co-dimension 1 invariant manifolds when intersected with the energy surface. They do not have the property of being compact and boundaryless like the NHIMs we have discussed above. We would not expect this since (almost) all trajectories that enter $\mathcal{L}$ leave $\mathcal{L}$. These co-dimension 1 invariant manifolds intersect the boundary of $\mathcal{L}$, and their projection into the $q_1 - p_1 - q_2 - p_2$ space gives the coordinate axes shown in figure 2. This is consistent with our description of trajectories that enter and exit $\mathcal{L}$ through the use of the integrals I_1 and I_2.

While the existence of co-dimension 1 invariant manifolds in phase space associated with index 1 or index 2 saddles is conceptually appealing, practically, their main use derives from the integrable structure of the normal form and the expression of Hamilton's equation using this integrability (e.g. (21)). This expression allows for a decoupling of the dynamics into unbounded motion (the 'reactive modes' described by I_1 and I_2) and bounded motion (the

'bath modes' described by $I_k, k = 3, \ldots, n$). The 'reactive dynamics' is described by a reduced dimensional system and the dynamics in this system is integrable and characterized by the level sets of these integrals. The relevant co-dimension 1 invariant manifolds drop out of this description naturally.

In the earlier work related to index 1 saddles in [8, 9], the integrable structure was not emphasized and the use of the integrals was not developed. Rather, the emphasis was on the use of the normal form in discovering the phase-space structures. It was hoped that a by-product of the normal form computations might be useful and intuitive visualization methods of the kind that have proved extremely useful and insightful for 2 DoF systems. However, visualization schemes for the invariant manifolds governing reaction in systems with 3 and more DoF have thus far been of limited value. In [12], attempts were made to visualize the phase-space invariant manifolds governing (planar) HCN isomerization in three dimensions by projecting the manifolds into the three-dimensional configuration space. In this case, the dividing surface (in a fixed energy surface) was four dimensional with its equator, the NHIM, three dimensional. It was difficult to interpret their projections into the three-dimensional configuration space (visually, they did not appear significantly different). Moreover, reversibility of Hamilton's equations in this case implies that the projections of the four-dimensional stable and unstable manifolds into configuration space are identical. While the visualization of high-dimensional phase-space structures is an appealing concept, we believe that the dimensional reduction afforded by integrability of the normal form in a neighborhood of the equilibrium point is a much more powerful tool for understanding reactive phenomena. It provides a precise notion of dimensional reduction to the number of DoFs undergoing 'reactive behavior' (i.e., the DoF for which there is the possibility of leaving a neighborhood of the equilibrium point). The significance of integrability was emphasized in [16] where it was also shown how the phase-space structures can be expressed in terms of the integrals (which is what we have essentially done here). While their utility for higher dimensional visualization remains to be demonstrated, for index 1 saddles the dividing surface plays an important role for a certain type of sampling [11, 13, 14] and the NHIM plays a role in determining the flux through the dividing surface. We will discuss this in more detail in section 7.

5.4. Higher index saddles

Once the generalization from index 1 to index 2 saddles has been made, generalization to higher index saddles is straightforward. For an n DoF deterministic, the time-independent Hamiltonian system, an index k saddle ($1 \leqslant k \leqslant n$) of the potential energy surface corresponds to an equilibrium point of Hamilton's equations where the matrix associated with the linearization of Hamilton's equations about the equilibrium point has k pairs of real eigenvalues and $n-k$ pure imaginary pairs of eigenvalues. Assuming that appropriate generic non-resonance assumptions on the real and imaginary eigenvalues hold, then a transformation to an integrable Poincaré–Birkhoff normal form in a neighborhood of the equilibrium point as described above can be carried out. For energies above the equilibrium point, the system has k integrals describing 'reactive' dynamics (i.e., trajectories that can enter and leave a neighborhood of the equilibrium point) and $n-k$ integrals describing 'bath modes' (i.e., bounded motions in a neighborhood of the equilibrium point). Hence integrability allows the reactive dynamics to be studied with a $2k$-dimensional reduced system with the k reactive integrals providing precise information about the nature of trajectories that pass through a neighborhood of the equilibrium point. Moreover, for energies above the saddle, the system has a NHIM of dimension $2n-2k-1$ having $(2n-k-1)$-dimensional stable and unstable

manifolds in the $(2n-1)$-dimensional energy surface. In the neighborhood of the equilibrium point, there are 4^k qualitatively distinct trajectory classes.

5.5. Quantitative application of Poincaré–Birkhoff normal form theory

Applying the formalism for higher index saddles to realistic molecular systems requires software that computes the normal form Hamiltonian, extracts the integrals of the motion and computes the coordinate transformation (and its inverse) from the original physical coordinates to the normal form coordinates, all to sufficiently high order to yield the desired accuracy (and accuracy must be assessed by a battery of tests at all points of the calculation). Software to carry out this program is available at http://lacms.maths.bris.ac.uk/publications/software/index.html.

6. Index 2 saddles and isomerization dynamics

A number of possible contexts in which index 2 saddles might be important have already been discussed in section 1. It is however useful to specify the possible dynamical role of index 2 saddles more precisely. We consider two examples: first, the dynamical definition of stepwise (sequential) versus concerted isomerization mechanisms on a multi-well potential surface; second, the classification of reactive trajectories in a system in which there are two distinct transition states. In the latter case, our analysis of dynamics in the vicinity of the index 2 saddle suggests a rigorous identification of so-called 'non-MEP' [57–62] or 'roaming' trajectories [63–68] based on phase-space structures.

It should be noted that the partitioning of phase space we discuss is local, that is, restricted to the vicinity of the index 2 saddle.

6.1. Stepwise versus concerted isomerization

Index 2 saddles are of dynamical significance in the identification of sequential versus concerted isomerization mechanisms in the case of multiple well isomerizations.

6.1.1. Stepwise versus concerted isomerization in 2 DoF. Consider a system with two coordinates $(\bar{q}_1, \bar{q}_2)$ having a multiwell potential surface $v(\bar{q}_1, \bar{q}_2)$ of the kind shown schematically in figure 3 [12]. Such a surface can describe, for example, conformational energies as a function of internal angles [40] or internal rotation/inversion potentials [41]. (See, for example, figure 1 in [40].)

The model potential shown has four minima. Each potential minimum is given a symbolic label according to the quadrant of the $(\bar{q}_1, \bar{q}_2)$ plane in which it is located. For example, minimum $(--)$ is located in the quadrant $(\bar{q}_1 < 0, \bar{q}_2 < 0)$.

The minima are connected by index 1 saddles, each denoted by the symbol ‡. At higher energy, in the middle of the potential surface, sits an index 2 saddle, denoted by ‡‡ (the 'hilltop'). (We locate the index 2 saddle at the coordinate origin, $(\bar{q}_1, \bar{q}_2) = (0, 0)$ and take the value of the potential at the hilltop to be zero, $v(0, 0) = 0$.)

For total energies $E < 0$, the system can only make transitions between minima by passing through the phase-space dividing surfaces (transition states) associated with the index 1 saddles (NHIMs). For such energies, we can define the distinct bound (reactant) regions of phase space in the usual way and describe the isomerization kinetics in terms of the associated phase-space volumes and flux through phase-space dividing surfaces associated with the index 1 saddles.

[12] We assume a kinetic energy of standard form, separable and quadratic in the conjugate momenta $(\bar{p}_1, \bar{p}_2)$.

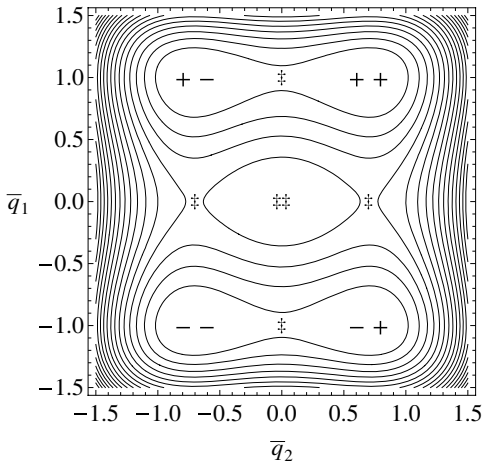

Figure 3. Contour plot of a model 2 DoF potential having four minima, four index 1 saddles (‡) and one index 2 saddle (‡‡).

Classes of isomerizing trajectories associated with particular transitions between wells can be denoted symbolically: for example, trajectories of type $(-+;\,--)$ start in the well $(--)$ and pass to the well $(-+)$ through the appropriate dividing surface.

It is clear that, for $E < 0$, the only way the system can pass from well $(--)$ to well $(++)$, say, is by a *stepwise* mechanism: a sequence of isomerizations such as $(+-;\,--)$ followed by $(++;\,+-)$ is required.

By contrast, for $E > 0$, trajectories are in principle able to 'roam' around on the potential surface. In addition to the sequential mechanism just described, there is another possibility, namely, a hilltop crossing or *concerted* mechanism, where, for the example just discussed, a trajectory simply passes 'directly' from well $(--)$ to well $(++)$ without undergoing the stepwise isomerization process which is necessary for $E < 0$.

It is then natural to ask: how can we distinguish between these mechanisms in a dynamically rigorous way? It is not sufficient to analyze trajectories in configuration space, as both sequentially isomerizing and hilltop crossing trajectories will pass close to the index 2 saddle.

The key to dynamical analysis of isomerizing trajectories is the symbolic trajectory classification introduced previously. We imagine that the saddle–saddle normal form has been obtained in the vicinity of the index 2 saddle. This means, in particular, that a (nonlinear, in general) invertible symplectic transformation T has been obtained relating physical coordinates $(\bar{q}_1, \bar{p}_1, \bar{q}_2, \bar{p}_2)$ and normal form coordinates (q_1, p_1, q_2, p_2) [9, 16]:

$$(\bar{q}, \bar{p}) = T(q, p). \tag{22}$$

In a phase-space neighborhood of the saddle–saddle equilibrium, it is therefore possible to use the inverse transformation $(q, p) = T^{-1}(\bar{q}, \bar{p})$ to determine the normal form coordinates along a given trajectory. Given these normal form coordinates and the approximate integrability of the motion in the vicinity of the index 2 saddle, a trajectory with energy $E > 0$ can be classified according to the symbolic scheme developed previously.

For the particular kind of potential surface considered here, the symbolic classification scheme of trajectories using the normal form is precisely the desired classification scheme for isomerization behavior. For example, a trajectory of type $(+-;\,--)$ passes from well

$(--)$ to well $(+-)$, and so is part of a sequential isomerization process, while a trajectory of type $(++; --)$ is a hilltop crossing trajectory that, as determined by a rigorous phase-space criterion in the vicinity of the saddle–saddle equilibrium, passes directly from well $(--)$ to well $(++)$.

6.1.2. Stepwise versus concerted isomerization in 3 DoF. We now introduce a third mode: for simplicity, we first consider an uncoupled harmonic oscillator DoF. As discussed in section 3.3, there is now a saddle–saddle–center equilibrium. For given total energy E, there will be distinct regimes, depending on the partitioning of energy between mode 3 and the 2 DoF isomerizing subsystem.

If the total energy E is above that of the index 2 saddle, but there is sufficient energy in mode 3, then hilltop crossing isomerization is not possible in the 2 DoF subsystem. If on the other hand the amount of energy in mode 3 is small, then the 2 DoF subsystem can undergo both sequential and hilltop crossing isomerization. Isomerizing trajectories in the 3 DoF system can then be classified using the normal form including the center DoF as developed in section 3.3.

Suppose that mode 3 and the 2 DoF subsystem are now coupled. If we consider the behavior of trajectories initialized in a region of phase space with a large amount of energy in mode 3, a relevant question is: what is the mechanism by which the system will pass from one potential minimum to another, given that the minima in question are separated by more than one saddle at low energies?

Intuitively, there are two possibilities: if significant energy transfer between mode 3 and the 2 DoF subsystem does not occur, then the system simply passes from one well to the other in a sequential fashion. If however energy transfer occurs between mode 3 and the 2 DoF isomerizing subsystem, it is possible that sufficient energy can pass into the 2 DoF subsystem so that trajectories can isomerize via the hilltop crossing mechanism. In this case, hilltop isomerization is mediated by the additional mode.

These dynamical alternatives can in principle be distinguished using the transformation to normal form coordinates in the vicinity of the saddle–saddle–center equilibrium (cf section 3.3).

6.2. Competing transition states and non-MEP mechanisms

We now discuss a second example where analysis of the phase-space structure in the vicinity of an index 2 saddle is potentially useful for obtaining deeper mechanistic understanding of an isomerization reaction.

Consider the model 2 DoF potential shown in figure 4. This potential has two minima, two index 1 saddles (having different energies) and one index 2 saddle (energy $E = 0$). The index 2 saddle sits between the two index 1 saddles (as per Murrell–Laidler [35]). (See, for example, the double proton transfer reaction in napthazarin, scheme 14 in [37].)

At total energies $E < 0$, the system can pass from one well to another through either of two transition states; in the example shown, the transition state associated with the index 1 saddle at $\bar{q}_2 < 0$ has lower energy, and hence is associated with the 'minimum energy path' mechanism.

At energies above that of the higher energy TS (denoted by channel 2), there may exist some kind of dynamical competition between transition states: the lower energy TS (channel 1) might be narrow (small flux), while the higher energy TS (channel 2) might be broader (larger flux).

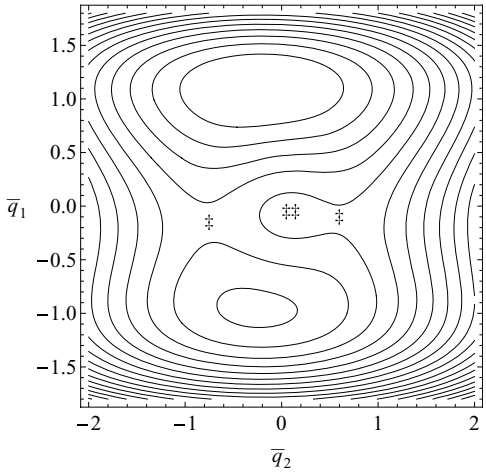

Figure 4. Contour plot of a model 2 DoF potential having two minima, two index 1 saddles (‡) and one index 2 saddle (‡‡).

For energies above the hilltop, $E > 0$, there are in principle three possibilities: trajectories can isomerize via channel 1, via channel 2, or they can isomerize by 'passage over the hilltop'.

Once again, the symbolic classification of trajectories in the vicinity of the saddle–saddle equilibrium enables the three classes of trajectory to be rigorously identified. Trajectories of class $(+-;\,--)$ correspond to the first mechanism (channel 1), of class $(++;\,-+)$ to the second mechanism (channel 2), while trajectories of class $(+-;\,-+)$ or $(++;\,--)$ are associated with the hilltop crossing isomerization.

All isomerizing trajectories except those of class $(+-;\,--)$ can therefore be labeled 'non-MEP' trajectories [57–62], and can tentatively be identified as 'roaming' trajectories [63–68]. Numerical studies of the dynamical significance of this local phase-space classification of trajectories are currently in progress.

7. Summary and conclusions

In this paper, we have analyzed the phase-space structure in the vicinity of an equilibrium point associated with an index 2 saddle or 'hilltop' on a potential energy surface (index 2 saddle). For the case of model quadratic Hamiltonians, we have shown that the behavior of trajectories passing through a phase-space neighborhood of the equilibrium is fully characterized by the value of associated integrals of the motion. We have introduced a symbolic classification of trajectories in the vicinity of the saddle–saddle equilibrium, where the symbolic representation of trajectory classes is directly related to the nature of the associated hilltop crossing dynamics. For the general case where nonlinear terms are present in the Hamiltonian, Poincaré–Birkhoff normal form theory provides a constructive procedure for obtaining an integrable approximation to the full Hamiltonian in the vicinity of the equilibrium, allowing a corresponding classification of trajectories to be made in the general case.

As for the case of index 1 saddles, normally hyperbolic invariant manifolds (NHIMs) associated with index 2 saddles are an important phase-space structure, and we have described the role they play in phase-space transport in the vicinity of index 2 saddles. In particular, we have shown that the normal form transformation enables co-dimension 1 surfaces to be

defined in phase space; these surfaces serve to partition phase space in the vicinity of the saddle–saddle equilibrium into regions corresponding to distinct trajectory types.

Two examples of the importance of index 2 saddles in problems of chemical dynamics were considered. First, isomerization on a potential energy surface with multiple symmetry equivalent minima; second, isomerization in a system having two potential minima connected by two distinct transition states associated with conventional index 1 saddles, with an index 2 saddle situated between the two index 1 saddles. We suggest that classification of different classes of reactive trajectories in the vicinity of the index 2 saddle enables a rigorous definition of non-MEP trajectories to be given in terms of local phase-space structure.

To conclude, we list several topics that we believe merit further investigation for the case of index 2 saddles.

Reaction coordinates. For the case of index 1 saddles, a natural definition of a phase-space reaction coordinate is obtained by putting all of the energy into the reactive mode [12, 16], i.e., for energy $H = E$, and the Hamiltonian expressed as a function of the integrals, we set

$$H(I_1, 0, \ldots, 0) = E. \tag{23}$$

This condition defines a path in the 'reactive plane' defined by q_1 and p_1 in normal form coordinates, which can then be mapped back into the original physical coordinates by the normal form transformation.

For the case of an index 2 saddle, we have two reactive modes, described by the integrals I_1 and I_2, and a four-dimensional 'reactive space' defined by the coordinates $q_1 - p_1 - q_2 - p_2$. Can dynamically significant paths analogous to that for the index 1 saddle be defined in this reactive space?

Activated complex. For index 1 saddles, the NHIM has the interpretation as the 'activated complex' [9, 16]. Do the NHIMs associated with index k saddles $1 < k \leqslant n$ have a similar chemical significance?

Flux. For the case of index 1 saddles, the NHIM is the 'boundary' of the forward and backward dividing surfaces. The magnitudes of the fluxes across each of these dividing surfaces are equal and, using the Stokes theorem, are expressed as the integral of an appropriate quantity over the NHIM, equal to the volume in the space of 'bath modes' enclosed by the contour defined by $H(0, I_2, \ldots, I_n) = E$ [11].

For index 2 (and higher) saddles, it is natural to ask whether or not there is any chemical significance to the volume in the space of 'bath modes' enclosed by the contour defined by $H(0, 0, I_3, \ldots, I_n) = E$.

Gap times and sampling. Can one develop a useful gap time formalism [82–84] to characterize rates of passage in and out of phase-space regions defined by the co-dimension 1 surfaces associated with index 2 saddles (and higher)?

Related to the gap time formalism, it has been shown that the dividing surface provided by the normal form provides a natural surface on which to sample initial conditions for trajectory calculations that yield quantities of physical interest such as the reactant volume or dissociation rate [13, 84]. Does the normal form associated with index 2 saddles yield manifolds on which a similar trajectory sampling strategy can be implemented?

The manifolds $q_1 = 0$, $p_1 = 0$ $q_2 = 0$ and $p_2 = 0$, a new type of NHIM? We have been careful *not* to refer to the co-dimension 1 invariant manifolds defined by $q_1 = 0$, $p_1 = 0$, $q_2 = 0$ and $p_2 = 0$ as 'NHIMs'. There are two reasons for this. The first is that they are not of the character of the NHIMs associated with index 1 saddles, i.e., compact and boundaryless (diffeomorphic to spheres), having (invariant) stable and unstable manifolds (locally) partitioning the energy

surface into reactants and products, and 'persistent under perturbations' (practically, this means that the manifolds maintain their character for a range of energy above that of the saddle). The second is that they do *not* immediately satisfy the hypotheses of the existing normally hyperbolic invariant manifold theorems [79]. This latter point deserves more discussion. Roughly speaking, the property of 'normal hyperbolicity' means that, under linearized dynamics, the magnitude of the growth and decay of vectors normal to the manifolds dominate the magnitude of the growth and decay of vectors tangent to the manifold. The manifolds under consideration are obtained by setting one coordinate to zero. Therefore, the growth of vectors under the linearized dynamics in the direction of the coordinate set to zero describes the normal dynamics, and it is a simple matter to verify that in this direction vectors are either exponentially growing or decaying (depending on the manifold under consideration). The problem is that there will also be directions tangent to the manifold that are exponentially growing or decaying. Additionally, these manifolds are *not* compact and boundaryless. Sometimes this difficulty can be dealt with through a consideration of 'overflowing' or 'inflowing' invariance (see [79] for examples and related references). Nevertheless, the manifolds do exist for the normal form truncated at *any* order, and this is sufficient for our purposes. Using this property and the ideas and setting just described, it may be possible to prove something like a 'persistence theorem for normally hyperbolic invariant manifolds' for this setting, but we do not pursue that problem here.

Addressing several of these issues will require globalizing the invariant manifolds obtained in the vicinity of the saddle–saddle equilibrium. Indeed, globalization constitutes an outstanding challenge for the theory of the dynamics associated with higher index saddles.

Acknowledgments

SW acknowledges the support of the Office of Naval Research Grant No N00014-01-1-0769. GSE and SW both acknowledge the stimulating environment of the NSF sponsored Institute for Mathematics and its Applications (IMA) at the University of Minnesota, where this manuscript was completed.

Appendix. Phase-space geometry and transport associated with an *n* DoF quadratic Hamiltonian of a saddle–saddle–center–. . .–center equilibrium point

The following quadratic Hamiltonian describes the dynamics near a saddle–saddle–center–. . .–center stability type equilibrium point located at the origin:

$$H_{n-\text{quad}} = \lambda_1 q_1 p_1 + \lambda_2 q_2 p_2 + \sum_{i=3}^{n} \frac{\omega_i}{2}\left(q_i^2 + p_i^2\right), \tag{A.1}$$

with associated Hamilton's equations:

$$\dot{q}_1 = \frac{\partial H_{n-\text{quad}}}{\partial p_1} = \lambda_1 q_1, \tag{A.2a}$$

$$\dot{p}_1 = -\frac{\partial H_{n-\text{quad}}}{\partial q_1} = -\lambda_1 p_1, \tag{A.2b}$$

$$\dot{q}_2 = \frac{\partial H_{n-\text{quad}}}{\partial p_2} = \lambda_2 q_2, \tag{A.2c}$$

$$\dot{p}_2 = -\frac{\partial H_{n-\text{quad}}}{\partial q_2} = -\lambda_2 p_2, \tag{A.2d}$$

$$\dot{q}_i = \frac{\partial H_{n-\text{quad}}}{\partial p_i} = \omega_i p_i, \qquad i = 3, \ldots, n, \tag{A.2e}$$

$$\dot{p}_i = -\frac{\partial H_{n-\text{quad}}}{\partial q_i} = -\omega_i q_i, \qquad i = 3, \ldots, n. \tag{A.2f}$$

It is straightforward to verify that $I_1 = q_1 p_1$, $I_2 = q_2 p_2$, $I_k = \frac{\omega_k}{2}\left(q_k^2 + p_k^2\right)$, $k = 3, \ldots, n$ are (independent) integrals of the motion for (A.1). As previously, we define a neighborhood of the saddle–saddle–center equilibrium point in phase space as follows:

$$\mathcal{L} \equiv \{(q_1, p_1, \ldots, q_n, p_n) \mid |q_i| \leqslant \varepsilon_i, |p_i| \leqslant \varepsilon_i, i = 1, \ldots, n\}, \tag{A.3}$$

for appropriately chosen $\varepsilon_i > 0, i = 1, \ldots, n$. Again, the fact that Hamilton's equations are separable, and that the motion of q_k and p_k is bounded, $k = 3, \ldots, n$ means that the issue of trajectories entering $\mathcal{L}$ and exiting $\mathcal{L}$ depends entirely on the behavior of the (q_1, p_1, q_2, p_2) components of a trajectory and, as a consequence of separability, this behavior is exactly as described in section 3.2.

As for the 3 DoF case considered in section 3, the equilibrium point is located at the origin and has zero energy, and we will consider geometric structures in the energy surface for positive energies:

$$H_{n-\text{quad}} = \lambda_1 q_1 p_1 + \lambda_2 q_2 p_2 + \sum_{k=3}^{n} \frac{\omega_k}{2}\left(q_k^2 + p_k^2\right) = E > 0. \tag{A.4}$$

It is clear from (A.4) that $q_1 = p_1 = q_2 = p_2 = 0$ is a two-dimensional invariant manifold in the $2n$-dimensional phase space. Using (A.4), its intersection with the $(2n-1)$-dimensional energy surface is given by

$$\sum_{k=3}^{n} \frac{\omega_k}{2}\left(q_k^2 + p_k^2\right) = E > 0. \tag{A.5}$$

This is the equation for a $(2n-5)$-dimensional sphere, S^{2n-5}, in the energy surface; as above, it is an example of a NHIM [7, 79]. The coordinates q_1, p_1, q_2, p_2 can be viewed as coordinates for the normal directions of the NHIM, and it follows from the nature of the asymptotic (in time) behavior of these coordinates (see (A.2)) that this NHIM has a $(2n-3)$-dimensional stable manifold and a $(2n-3)$-dimensional unstable manifold in the $(2n-1)$-dimensional energy surface.

References

[1] Wigner E P 1938 The transition state method *Trans. Faraday Soc.* **34** 29–40
[2] Keck J C 1967 Variational theory of reaction rates *Adv. Chem. Phys.* **XIII** 85–121
[3] Pechukas P 1981 Transition state theory *Ann. Rev. Phys. Chem.* **32** 159–77
[4] Truhlar D G, Hase W L and Hynes J T 1983 Current status of transition-state theory *J. Phys. Chem.* **87** 2664–82
[5] Anderson J B 1995 Predicting rare events in molecular dynamics *Adv. Chem. Phys.* **XCI** 381–431
[6] Truhlar D G, Garrett B C and Klippenstein S J 1996 Current status of transition-state theory *J. Phys. Chem.* **100** 12711–800
[7] Wiggins S 1990 On the geometry of transport in phase space: I. Transport in k-degree-of-freedom Hamiltonian systems, $2 \leqslant k < \infty$ *Physica* D **44** 471–501
[8] Wiggins S, Wiesenfeld L, Jaffe C and Uzer T 2001 Impenetrable barriers in phase-space *Phys. Rev. Lett.* **86** 5478–81
[9] Uzer T, Jaffe C, Palacian J, Yanguas P and Wiggins S 2002 The geometry of reaction dynamics *Nonlinearity* **15** 957–92
[10] Waalkens H, Burbanks A and Wiggins S 2004 A computational procedure to detect a new type of high-dimensional chaotic saddle and its application to the 3D Hill's problem *J. Phys. A: Math. Gen.* **37** L257–65

[11] Waalkens H and Wiggins S 2004 Direct construction of a dividing surface of minimal flux for multi-degree-of-freedom systems that cannot be recrossed *J. Phys. A: Math. Gen.* **37** L435–45
[12] Waalkens H, Burbanks A and Wiggins S 2004 Phase space conduits for reaction in multidimensional systems: HCN isomerization in three dimensions *J. Chem. Phys.* **121** 6207–25
[13] Waalkens H, Burbanks A and Wiggins S 2005 Efficient procedure to compute the microcanonical volume of initial conditions that lead to escape trajectories from a multidimensional potential well *Phys. Rev. Lett.* **95** 084301
[14] Waalkens H, Burbanks A and Wiggins S 2005 A formula to compute the microcanonical volume of reactive initial conditions in transition state theory *J. Phys. A: Math. Gen.* **38** L759–68
[15] Schubert R, Waalkens H and Wiggins S 2006 Efficient computation of transition state resonances and reaction rates from a quantum normal form *Phys. Rev. Lett.* **96** 218302
[16] Waalkens H, Schubert R and Wiggins S 2008 Wigner's dynamical transition state theory in phase space: classical and quantum *Nonlinearity* **21** R1–R118
[17] MacKay R S 1990 Flux over a saddle *Phys. Lett.* A **145** 425–7
[18] Komatsuzaki T and Berry R S 2000 Local regularity and non-recrossing path in transition state—a new strategy in chemical reaction theories *J. Mol. Struct.: THEOCHEM* **506** 55–70
[19] Komatsuzaki T and Berry R S 2002 Chemical reaction dynamics: many-body chaos and regularity *Adv. Chem. Phys.* **123** 79–152
[20] Toda M 2002 Dynamics of chemical reactions and chaos *Adv. Chem. Phys.* **123** 153–98
[21] Wiesenfeld L, Faure A and Johann T 2003 Rotational transition states: relative equilibrium points in inelastic molecular collisions *J. Phys. B: At. Mol. Opt. Phys.* **36** 1319–35
[22] Wiesenfeld L 2004 Local separatrices for Hamiltonians with symmetries *J. Phys. A: Math. Gen.* **37** L143–9
[23] Wiesenfeld L 2004 Dynamics with a rotational transition state *Few-Body Syst.* **34** 163–8
[24] Komatsuzaki T, Hoshino K and Matsunaga Y 2005 Regularity in chaotic transitions on multi-basin landscapes *Adv. Chem. Phys.* B **130** 257–313
[25] Jaffé C, Shinnosuke K, Palacian J, Yanguas P and Uzer T 2005 A new look at the transition state: Wigner's dynamical perspective revisited *Adv. Chem. Phys.* A **130** 171–216
[26] Wiesenfeld L 2005 Geometry of phase space transition states: many dimensions, angular momentum *Adv. Chem. Phys.* A **130** 217–65
[27] Gabern F, Koon W S, Marsden J E and Ross S D 2005 Theory and computation of non-RRKM lifetime distributions and rates in chemical systems with three or more degrees of freedom *Physica* D **211** 391–406
[28] Gabern F, Koon W S, Marsden J E and Ross S D 2006 Application of tube dynamics to non-statistical reaction processes *Few-Body Syst.* **38** 167–72
[29] Shojiguchi A, Li C B, Komatsuzaki T and Toda M 2008 Dynamical foundation and limitations of statistical reaction theory *Commun. Nonlinear Sci. Numer. Simul.* **13** 857–67
[30] Heidrich D and Quapp W 1986 Saddle points of index 2 on potential energy surfaces and their role in theoretical reactivity investigations *Theor. Chim. Acta* **70** 89–98
[31] Mezey P G 1987 *Potential Energy Hypersurfaces* (Amsterdam: Elsevier)
[32] Wales D J 2003 *Energy Landscapes* (Cambridge: Cambridge University Press)
[33] Jensen F 1998 Transition structure optimization techniques *Encyclopedia of Computational Chemistry* ed P V R Schleyer (New York: Wiley) pp 3114–23
[34] Minyaev R M 1991 Molecular structure and global description of the potential energy surface *J. Struct. Chem.* **32** 559–89
[35] Murrell J N and Laidler K J 1968 Symmetries of activated complexes *Trans. Faraday Soc.* **64** 371–7
[36] Wales D J and Berry R S 1992 Limitations of the Murrell–Laidler theorem *J. Chem. Soc. Faraday Trans.* **88** 543–4
[37] Minyaev R M 1994 Reaction path as a gradient line on a potential energy surface *Int. J. Quantum Chem.* **49** 105–27
[38] Minyaev R M 1994 Gradient lines on multidimensional potential energy surfaces and chemical reaction mechanisms *Russ. Chem. Rev.* **63** 883–903
[39] Minyaev R M, Getmanskii I V and Quapp W 2004 A second-order saddle point in the reaction coordinate for the isomerization of the NH_5 complex: Ab initio calculations *Russ. J. Phys. Chem.* **78** 1494–8
[40] Minyaev R M 1995 Correlated internal rotations of CH_3 groups in dimethyl ether and BH_2 groups in diborylmethylene *Russ. J. Phys. Chem.* **69** 1463–71
[41] Minyaev R M and Lepin E A 1997 Internal rotation in the H_2BNH_2 molecule *Russ. J. Phys. Chem.* **71** 1449–53
[42] Bryantsev V S, Firman T K and Hay B P 2005 Conformational analysis and rotational barriers of alkyl- and phenyl-substituted urea derivatives *J. Phys. Chem.* A **109** 832–42

[43] Fau S and Frenking G 1995 Anti van't Hoff/Le Bel geometries of boron compounds. A theoretical study of classical and non-classical isomers of B_2CH_4, B_2NH_3 and B_2OH_2 *Theochem J. Mol. Struct.* **338** 117–30
[44] Salem L 1971 Narcissistic reactions: synchronism versus nonsynchronism in automerizations and enatiomerizations *Acc. Chem. Res.* **4** 322–8
[45] Carpenter B K 2004 Potential energy surfaces and reaction dynamics *Reactive Intermediate Chemistry* ed R A Moss, M S Platz and M Jones Jr (New York: Wiley) pp 925–60
[46] Meroueh S O, Wang Y F and Hase W L 2002 Direct dynamics simulations of collision and surface-induced dissociation of N-protonated glycine. Shattering fragmentation *J. Phys. Chem.* A **106** 9983–92
[47] Cavagna A, Giardini I and Parisi G 2001 Role of saddles in mean-field dynamics above the glass transition *J. Phys. A: Math. Gen.* **34** 5317–26
[48] Cavagna A 2001 Fragile versus strong liquids: a saddles-ruled scenario *Europhys. Lett.* **53** 490–6
[49] Doye J P K and Wales D J 2002 Saddle points and dynamics of Lennard–Jones clusters, solids, and supercooled liquids *J. Chem. Phys.* **116** 3777–88
[50] Wales D J and Doye J P K 2003 Stationary points and dynamics in high-dimensional systems *J. Chem. Phys.* **119** 12409–16
[51] Angelini L, Ruocco G and Zamponi F 2003 Saddles and dynamics in a solvable mean-field model *J. Chem. Phys.* **118** 8301–6
[52] Shell M S, Debenedetti P G and Panagiotopoulos A Z 2004 Saddles in the energy landscape: extensivity and thermodynamic formalism *Phys. Rev. Lett.* **92** 035506
[53] Grigera T S 2006 Geometrical properties of the potential energy of the soft-sphere binary mixture *J. Chem. Phys.* **124** 064502
[54] Coslovich D and Pastore G 2007 Understanding fragility in supercooled Lennard–Jones mixtures: II. Potential energy surface *J. Chem. Phys.* **127** 124505
[55] Angelini L, Ruocco G and Zamponi F 2008 Role of saddles in topologically driven phase transitions: the case of the d-dimensional spherical model *Phys. Rev.* E **77** 052101
[56] Kastner M 2008 Phase transitions and configuration space topology *Rev. Mod. Phys.* **80** 167–87
[57] Mann D J and Hase W L 2002 Ab initio direct dynamics study of cyclopropyl radical ring-opening *J. Am. Chem. Soc.* **124** 3208–9
[58] Sun L P, Song K Y and Hase W L 2002 A S(N)2 reaction that avoids its deep potential energy minimum *Science* **296** 875–8
[59] Debbert S L, Carpenter B K, Hrovat D A and Borden W T 2002 The iconoclastic dynamics of the 1,2,6-heptatriene rearrangement *J. Am. Chem. Soc.* **124** 7896–7
[60] Ammal S C, Yamataka H, Aida M and Dupuis M 2003 Dynamics-driven reaction pathway in an intramolecular rearrangement *Science* **299** 1555–7
[61] Lopez J G, Vayner G, Lourderaj U, Addepalli S V, Kato S, Dejong W A, Windus T L and Hase W L 2007 A direct dynamics trajectory study of F−+ CH(3)OOH reactive collisions reveals a major Non-IRC reaction path *J. Am. Chem. Soc.* **129** 9976–85
[62] Lourderaj U, Park K and Hase W L 2008 Classical trajectory simulations of post-transition state dynamics *Int. Rev. Phys. Chem.* **27** 361–403
[63] Townsend D, Lahankar S A, Lee S K, Chambreau S D, Suits A G, Zhang X, Rheinecker J, Harding L B and Bowman J M 2004 The roaming atom: straying from the reaction path in formaldehyde decomposition *Science* **306** 1158–61
[64] Bowman J M 2006 Skirting the transition state, a new paradigm in reaction rate theory *Proc. Natl Acad. Sci. USA* **103** 16061–2
[65] Shepler B C, Braams B J and Bowman J M 2007 Quasiclassical trajectory calculations of acetaldehyde dissociation on a global potential energy surface indicate significant non-transition state dynamics *J. Phys. Chem.* A **111** 8282–5
[66] Shepler B C, Braams B J and Bowman J M 2008 'Roaming' dynamics in CH_3CHO photodissociation revealed on a global potential energy surface *J. Phys. Chem.* A **112** 9344–51
[67] Suits A G 2008 Roaming atoms and radicals: a new mechanism in molecular dissociation *Acc. Chem. Res.* **41** 873–81
[68] Heazlewood B R, Jordan M J T, Kable S H, Selby T M, Osborn D L, Shepler B C, Braams B J and Bowman J M 2008 Roaming is the dominant mechanism for molecular products in acetaldehyde photodissociation *Proc. Natl Acad. Sci. USA* **105** 12719–24
[69] Ball K D, Berry R S, Kunz R E, Li F Y, Proykova A and Wales D J 1996 From topographies to dynamics on multidimensional potential energy surfaces of atomic clusters *Science* **271** 963–6

[70] Berry R S 1996 Many-dimensional potential surfaces: what they imply and how to think about them *Int. J. Quantum Chem.* **58** 657–70
[71] Maxwell J C 1954 *A Treatise on Electricity and Magnetism* vol 1 (New York: Dover)
[72] Eckhardt B and Sacha K 2001 Wannier threshold law for two-electron escape in the presence of an external electric field *Europhys. Lett.* **56** 651–7
[73] Sacha K and Eckhardt B 2001 Pathways to double ionization of atoms in strong fields *Phys. Rev.* A **63** 043414
[74] Eckhardt B and Sacha K 2006 Classical threshold behaviour in a (1+1)-dimensional model for double ionization in strong fields *J. Phys. B: At. Mol. Opt. Phys.* **39** 3865–71
[75] Haller G 2009 Results announced in talk at American Physical Society Meeting, Pittsburgh, 18 March 2009
[76] Toda M 2005 Global aspects of chemical reactions in multidimensional phase space *Adv. Chem. Phys.* **130A** 337–99
[77] Li C B, Shojiguchi A, Toda M and Komatsuzaki T 2006 Definability of no-return transition states in the high-energy regime above the reaction threshold *Phys. Rev. Lett.* **97** 028302
[78] Toda M 2008 Dynamical reaction theory in multi-dimensional Hamilton systems *AIP Conf. Proc.* **1076** 245–54
[79] Wiggins S 1994 *Normally Hyperbolic Invariant Manifolds in Dynamical Systems* (Berlin: Springer)
[80] Waalkens H, Burbanks A and Wiggins S 2005 Escape from planetary neighborhoods *Mon. Not. R. Astron. Soc.* **361** 763–75
[81] Pollak E and Pechukas P 1978 Transition states, trapped trajectories, and bound states embedded in the continuum *J. Chem. Phys.* **69** 1218–26
[82] Thiele E 1962 Comparison of the classical theories of unimolecular reactions *J. Chem. Phys.* **36** 1466–72
[83] Dumont R S and Brumer P 1986 Dynamic theory of statistical unimolecular decay *J. Phys. Chem.* **90** 3509–16
[84] Ezra G S, Waalkens H and Wiggins S 2009 Microcanonical rates, gap times, and phase space dividing surfaces arXiv:0901.2721v1 [cond-mat.stat-mech]
[85] Eliasson H 1990 Normal forms for Hamiltonian systems with Poisson commuting integrals–elliptic case *Comment. Math. Helvetici* **65** 4–35
[86] Dullin H and Vu Ngoc S 2007 Symplectic invariants near hyperbolic–hyperbolic points *Regular Chaotic Dyn.* **12** 689–716